

An Evaluation of High Energy Density Battery Technologies for Substation Standby Applications

By:

Konstantinos Stamatis

A Thesis submitted to the Faculty of Graduate Studies of
The University of Manitoba
in partial fulfilment of the requirements of the degree of

MASTER OF SCIENCE

Department of Electrical and Computer Engineering
University of Manitoba
Winnipeg

Copyright © 2019 by Konstantinos Stamatis

Acknowledgments

I would like to sincerely thank Dr. Shaahin Filizadeh for his support, guidance and patience and for giving me the opportunity to work under his supervision. I would also like to thank Manitoba Hydro and MITACS for their funding and support.

I would like to give thanks to Barry Potapinski, Claude Berard, Colin McKenzie, Perry Kholi as well as all the people that assisted me in Stonewell training center. I would also like to thank Karim Abdel Hadi for too many things to name here. In addition I would like to thank Professor Polyzois and Professor Gole for being in the examining committee and for their great comments. Last but not least I would like to thank Veronica and my parents for all their support.

Abstract

The purpose of this thesis is to evaluate alternative battery chemistries for their usage as a substation battery bank. Lithium-ion and the previously untested (as a station back up) sodium-nickel-chloride batteries were chosen. Experimental setup for lithium-ion battery was built and tests were performed showing battery changes over the course of eighteen months. In addition to calendar aging an accelerated aging test using high temperatures was developed and tested. An experimental setup for sodium-nickel-chloride batteries was also designed with the batteries tested in substation conditions. Furthermore, capacity results from eighteen months of tests are discussed. The thesis is concluded by offering sizing procedures for sodium-nickel-chloride batteries and by developing asset health indexes and a maintenance framework based on reliability centered maintenance.

Table of Contents

Acknowledgments.....	ii
Abstract.....	iii
List of Figures	v
List of Tables	vi
Chapter 1 Introduction	1
1.1 Literature Review.....	4
1.2 Thesis Organization.....	6
Chapter 2 Battery Fundamentals.....	8
2.1 Battery Chemistries.....	11
2.1.1 Alkaline Batteries	12
2.1.2 Flow Batteries	13
2.1.3 Chemistries Comparison	14
2.2 Battery Models.....	15
2.3 Batteries in a Substation	22
Chapter 3 Lithium-Ion Batteries.....	25
3.1 Experimental Setup for Calendar Aging.....	27
3.2 Accelerated Aging Tests	31
3.3 Summary and Sizing	37
Chapter 4 Sodium-Nickel-Chloride Batteries	39
4.1 Experimental Setup.....	40
4.2 Implementing Sizing Practices	43
4.3 Developing Maintenance Guidelines	47
Chapter 5 Conclusion	53
References	56

List of Figures

Figure 1.1 Ready to move trailer	3
Figure 2.1 A battery cell	8
Figure 2.2 Substation battery bank setup.....	9
Figure 2.3 Flooded battery family	11
Figure 2.4 VRLA battery family.....	12
Figure 2.5 Station (133 V) and communication (48 V) mobile trailer.	13
Figure 2.6 Flow batteries cell.....	14
Figure 2.7 Energy density of different battery cells	14
Figure 2.8 Specific energy of different battery cells.....	15
Figure 2.9 Lead-acid vs sodium-nickel and lithium-ion footprints.	15
Figure 2.10 Ideal battery cell	16
Figure 2.11 Ideal battery discharge.....	16
Figure 2.12 Open circuit voltage	17
Figure 2.13 Resistance battery model.....	18
Figure 2.14 Experiment vs resistance battery model.....	19
Figure 2.15 Randall battery circuit	20
Figure 2.16 Shepherd model vs experimental data	21
Figure 2.17 Substation battery bank	22
Figure 2.18 Substation switchyard.....	22
Figure 3.1 Lithium-ion cell reactions.....	26
Figure 3.2 Stonewell experimental setup.....	27
Figure 3.3 Current-off discharge profile	28
Figure 3.4 Cell voltage during current-off test	29
Figure 3.5 1C discharge of new and aged batteries	30
Figure 3.6 Battery strings inside oven	32
Figure 3.7 BMS setup	32
Figure 3.8 Oven-charger-BMS setup.....	33
Figure 3.9 Discharge profile for the 83 V system.....	33
Figure 3.10 Cell voltage of the 83 V system (new batteries).....	34
Figure 3.11 Intense discharge current.....	35
Figure 3.12 Minimum cell voltage for batteries stored at 60°C	35
Figure 3.13 1C discharged batteries stored at 60°C.....	36
Figure 3.14 1C discharge of batteries stored at 60°C	37
Figure 4.1 Sodium-nickel-chloride cell	39
Figure 4.2 Representation of sodium-nickel-chloride internal components	40
Figure 4.3 Stonewell sodium-nickel-chloride experimental setup	41
Figure 4.4 Voltage (top) and Current Discharge Profile (bottom).....	42
Figure 4.5 Voltage (top) and Current Discharge Profile (bottom).....	43

List of Tables

Table 2.1 Peukert coefficients for some common battery chemistries	10
Table 2.2 Advantages of flooded cells.....	12
Table 2.3 Substation duty cycles	23
Table 4.1 Sodium-nickel-chloride capacities.....	42
Table 4.2 Capacity for different discharge rates.....	44
Table 4.3 Duty cycle example 66 kV station.....	44
Table 4.4 66 kV station sizing example.....	45
Table 4.5 Duty Cycle example.....	46
Table 4.6 115 kV station sizing example.....	46
Table 4.7 Mode cause task	50
Table 4.8 Maintenance tasks.....	51
Table 4.9 Asset health indexes.....	52

Chapter 1 Introduction

New battery designs employing non-traditional chemistries provide high energy densities that make them increasingly popular in automotive, data centre, and telecommunication industries. However, electric utilities have so far tended to eschew such technologies in favour of conventional lead-acid, and particularly Vented-Lead Acid (“VLA” or “flooded”) batteries.

Such reticence partly derives from these new technologies’ initial purchase prices, which can be up to three times more expensive than their conventional counterparts, along with the utilities’ negative historical experiences in adopting Valve-Regulated Lead Acid (“VRLA”) batteries approximately twenty years ago. Manufacturers at that time had marketed VRLAs to electric utilities as having comparable reliability and operational lifetimes to VLAs, but having the additional benefit of being maintenance-free and taking up less space. In reality, VRLA batteries were more expensive, less reliable, and required at least as much maintenance as their VLA counterparts that they were intended to replace. Moreover, VRLA batteries could not operate nearly as long as VLAs and failed open [38] instead of short, thereby causing a failure within a single cell to render the entire battery string inoperable. VRLAs have improved since their market introduction, but they nonetheless remain more expensive than VLAs and inferior in their performance for station standby applications, and the improvements have not been sufficient to diminish the wariness that many utilities continue to share for newly introduced technologies.

Utilities have thus been understandably reluctant to act as first adopters of new battery innovations and absorb the associated costs and risks. Nonetheless, newly-introduced high energy density batteries offer numerous practical advantages to their conventional lead-acid and nickel-cadmium counterparts. For example, they consume only 15% of the footprint of VLA batteries and can be quickly and safely installed by personnel without specialized training or expertise. They are also claimed to have long operational lifetimes, require virtually no maintenance (according to the manufacturers), and unlike VLA batteries, which begin to calcify after 4-6 months, remain functional even after prolonged periods of storage in an uncharged state. Moreover, in contrast to conventional batteries, whose cells generally must operate at similar capacities, a battery management system (BMS) actively manages the new technologies, thereby permitting both new and old battery cells to operate in tandem within a single string. This enables utilities to scale their power needs to suit evolving substation loads over time instead of either oversizing initial banks or reinstalling entirely new banks once loads increase beyond design capacity.

These potential benefits render the new battery technologies particularly attractive for deployment in specialized applications such as in isolated communities, where operations are hampered by high installation, transportation, and maintenance costs. These batteries also become highly competitive when their small footprints obviate the need to install expensive additional structures such as “Ready-to-Move (RTM)” (Figure 1.1) trailers in particularly cramped substations.



Figure 1.1.1 Ready to move trailer¹

The objective of this thesis is to select and test a reliable, cost effective battery system that would provide high power density and would meet the demands and expectation of a utility. Considering a company the size of Manitoba hydro, which has over 500 substations with each one

¹ Picture taken by Manitoba Hydro.

having at least one battery bank, choosing a battery that requires little to no maintenance is a top priority. To that effect, after reviewing different chemistries and their implementations the ones selected to be tested were a lithium-ion battery system supplied by SAFT and a sodium-nickel-chloride supplied by FZSONICK. A super capacitor system was also initially considered but since it contained VLA (that requires regular maintenance) batteries in its implementation it was deemed impractical. Through discharge tests as well as calendar and accelerated aging the suitability of the aforementioned battery systems for specific substation standby application was investigated.

1.1 Literature Review

There are different ways to develop a model for a battery, including mathematical models [1], electrochemical models [2], or equivalent-circuit models [3]; however, due to their complexity, electrochemical models are rarely used for real-time applications [4] and are too complicated for system-level studies. A great deal of research has been conducted on correctly identifying model parameters [2, 5]. Typically model parameters are calculated from test data on an actual battery pack [5]. A hybrid pulse power characterization test is often used to identify model parameters [6]. These parameters change with usage and/or time and their effect can be described as the aging of the battery.

The mechanisms behind the aging of Li-ion batteries have been well documented [7, 8]; however, there are many different types of Li-ion batteries [9] and some of them behave differently. Normally, a battery ages with cycling and/or time (calendar aging). Depending on the chemistry it may take a long period for the effects of aging to manifest themselves in the operating

characteristics of the battery. Work to accelerate the aging process has been done [10, 11] for certain chemistries and consists of both cycling aging and calendar aging.

Sodium-nickel-chloride batteries operate at temperatures in excess of 250 degree Celsius and comparison of high-temperature versus low-temperature performance has been documented [12], showing higher loss of voltage on cells cycled at a lower temperature. To the best of the author's knowledge there is no method that can artificially age this battery; however destructive tests have been performed where batteries were repeatedly cycled at their extremes of the recommended temperature range [2]. While charging and discharging at different temperatures might provide artificial aging, this type of tests could not be performed since the user is generally unable to alter the BMS. In addition, results of seven years of calendar aging have been published [33] indicating no capacity loss.

Although there has been prior work on lithium-ion batteries in substations [13, 14] there is still plenty of room for additional research work and especially on tests tailored for specific needs. In addition, although there has been work on modelling sodium-nickel-chloride batteries for energy storage [15], they have yet to be tested for usage as a substation battery bank.

Finally, due to the experimental nature of the thesis it is important to review regulatory and related standards. IEEE standard 450 [39] covers the maintenance, testing, and replacement for vented lead acid batteries and IEEE 485 [40] has the recommended sizing practices for lead-acid batteries. Although both documents offer a review of basic battery terminologies, the majority of their content is not applicable to either lithium or sodium-nickel batteries as they are different chemistries. Lastly NERC PRC 005 [41] covers battery testing and maintenance but does not include recommendations for either lithium or sodium chemistries. Since both chemistries

discussed in this thesis contain a battery management system, they would be able to pass the NERC regulation by having effective parameter monitoring.

1.2 Thesis Organization

Chapter 2 starts by offering a review of battery fundamentals as well as defining and explaining the most commonly used battery terminologies. A review of some commonly used battery chemistries for stationary application and some not so common chemistries is then presented. The chapter concludes by building a step-by-step battery model based on electrical components as well as one based on Shepherd's model. Finally, information regarding the batteries used in substation and their current sizing procedures is presented.

Chapter 3 starts by offering a detailed introduction to the lithium-ion chemistry, explaining its operating principles and differences between different types of lithium-ion batteries. The chapter continues with a review of the experimental setup and test procedures used in this study. Results from both calendar aging and artificially aged batteries are presented and analysed. The chapter concludes by offering sizing recommendations as well as technical observation obtained from two years of testing.

The focus of Chapter 4 is sodium-nickel-chloride batteries, starting with an overview of the chemistry fundamentals and cell constructions. The experimental setup is then presented together with the experimental results. A detailed analysis on how to size these batteries is then shown and a detailed sizing procedure is proposed. The chapter concludes by giving an overview of reliability centred maintenance, followed by the development of mode/cause/ task analysis and asset health indexes.

Chapter 5 enumerates this thesis contributions, including a list of publications, and gives a summary of major conclusions that may be drawn from the conducted work. Lastly recommendations for future work and research possibilities are presented.

Chapter 2 Battery Fundamentals

In this chapter a review of basic battery information will be presented followed by battery terminologies and a theoretical background necessary for understanding the rest of the thesis.

Batteries are defined by IEEE as “two or more cells electrically connected for producing electric energy” [16]. A cell is the smallest unit of a battery that delivers voltage. The amount of voltage delivered is dependent on which chemicals were to form the cell. A battery cell consists of a positive and negative electrode, a separator, and the electrolyte [17].

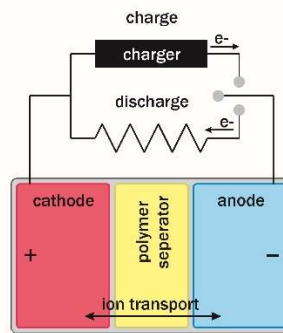


Figure 2.1 A battery cell²

There are two type of batteries - primary and secondary. Primary batteries have a one-way reaction between electrodes, and are depleted once used. A typical primary battery is the alkaline or zinc-air/carbon, but it also includes lithium chemistries. Utilities virtually always employ so-called secondary batteries, meaning that the chemical reactions that take place within the cell are reversible and that the battery may be recharged by passing a current through it in the direction opposite to that of its discharge. In this case, the battery, its charger, and the load are typically

² Picture modified from commons.wikimedia.org/wiki/File:Battery_with_polymer_separator.svg

connected in parallel, with the charger supplying both the load and the current required to keep the battery charged. The continuous, long-term, constant voltage required to balance a battery’s charging and discharging rate (and therefore to maintain a constant battery voltage) is called the float charge and a battery that is in this state is colloquially said to be “on float.” A battery only discharges to supply the load it is connected to if the charger’s output current is insufficient to supply the load itself or once the AC power fails. The most typical secondary battery chemistries are lead-acid, nickel-cadmium and lithium-ion.

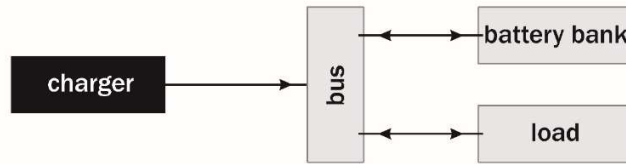


Figure 2.2 Substation battery bank setup

The battery’s capacity is the quantity of stored electrical energy that it can deliver from its completely charged state to its completely discharged state. Its state of charge (*SOC*) is its actual capacity expressed as a percentage of rated capacity, where capacity is normally expressed in Ampere-hours (Ah). Equation (2.1) shows a representation of *SOC* [18].

$$SOC = SOC(0) - \frac{1}{C} \int idt \tag{2.1}$$

where *SOC* is the current value of state of charge, *SOC*(0) is the initial value, *C* is the total battery capacity and $\int idt$ is the charge/discharge current change.

Because the capacity reduces as the rate at which it discharges (i.e., the rate at which electrical current is drawn from the battery) increases, it is often expressed in terms of a “C rate”,

which describes the amount of current that a battery can discharge/charge over an hour expressed as a fraction of its capacity. For example, an 80 Ah battery can provide 80 A for one hour or 40 A for two hours, and it is said to have a C-rate of $1C = 80 \text{ A}$ or $2C = 160 \text{ A}$ or $C/2 = 40 \text{ A}$. In reality depending on battery chemistry a battery's capacity is dependent on its discharge rate. Higher discharge rates lead to lower delivered capacity. This is described by Peukert law [19]

$$EC = C \left(\frac{C}{I \cdot t} \right)^{k-1} \quad (2.2)$$

where EC is the effective capacity at discharge rate I , t is time in hours, C is the rated capacity, and k is the Peukert coefficient. Table 2.1 shows Peukert's coefficients for various battery chemistries.

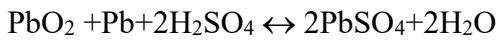
Table 2.1 Peukert coefficients for some common battery chemistries [20]

Battery type	Peukert coefficient
Flooded	1.20 to 1.60
Gel	1.10 to 1.25
Absorbent glass mat (AGM)	1.05 to 1.15

Peukert coefficients for lithium-ion batteries vary depending on the chemistry, and generally range between 1 to 1.10. For the battery chemistry that was used for testing in this thesis the Peukert coefficient was experimentally found to be between 1.02 and 1.04. This small variance can be explained by the current variations of the discharging equipment. Sodium nickel batteries do not have a constant Peukert coefficient as their capacity is dependent on discharge rate and can range from 1.01 to more than 1.2.

2.1 Battery Chemistries

Even though the focus of the thesis is on lithium-ion and sodium-nickel batteries a review of major stationary batteries chemistries is provided. Lead-acid batteries were first invented in 1859 by Gaston Plante [17]. A lead-acid battery consists of a positive PbO_2 plate and a negative Pb plate that are immersed in sulphuric acid (H_2SO_4). A separator is also used to keep the plates from touching. The overall chemical reaction [21] is as follows.



The typical nominal voltage of a lead-acid cell is 2 V. There are two main categories of lead acid batteries flooded (Figure 2.3) and VRLA (Figure 2.4). Both types of lead-acid batteries are fully rechargeable, contain sulphuric acid, and self-discharge. Although they both belong to the same battery family, flooded (VLA) and VRLA batteries have different advantages (Table 2.2).

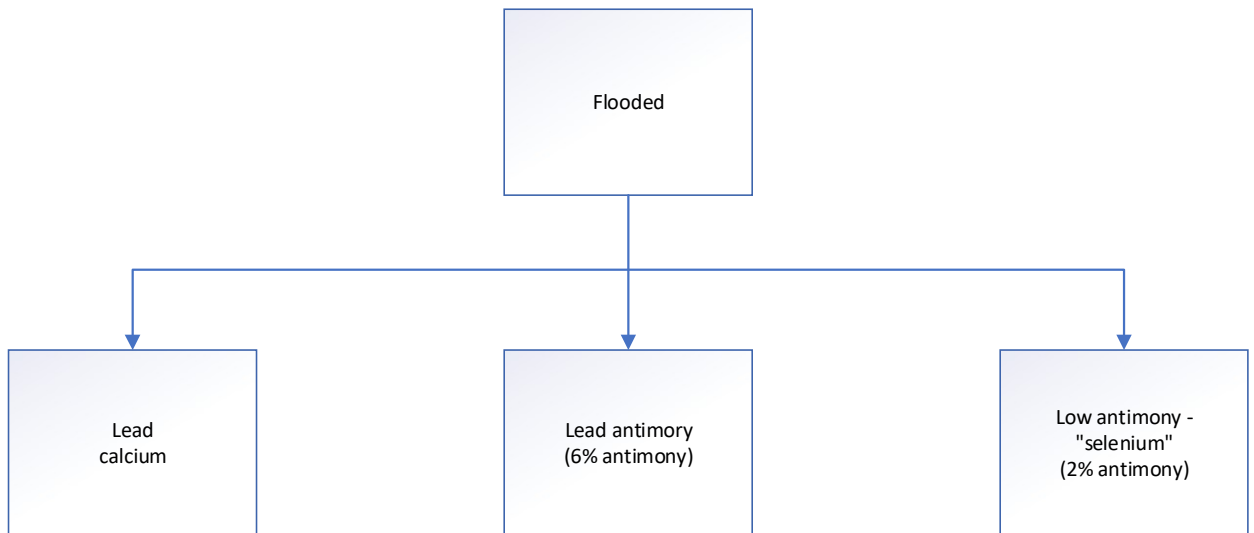


Figure 2.3 Flooded battery family

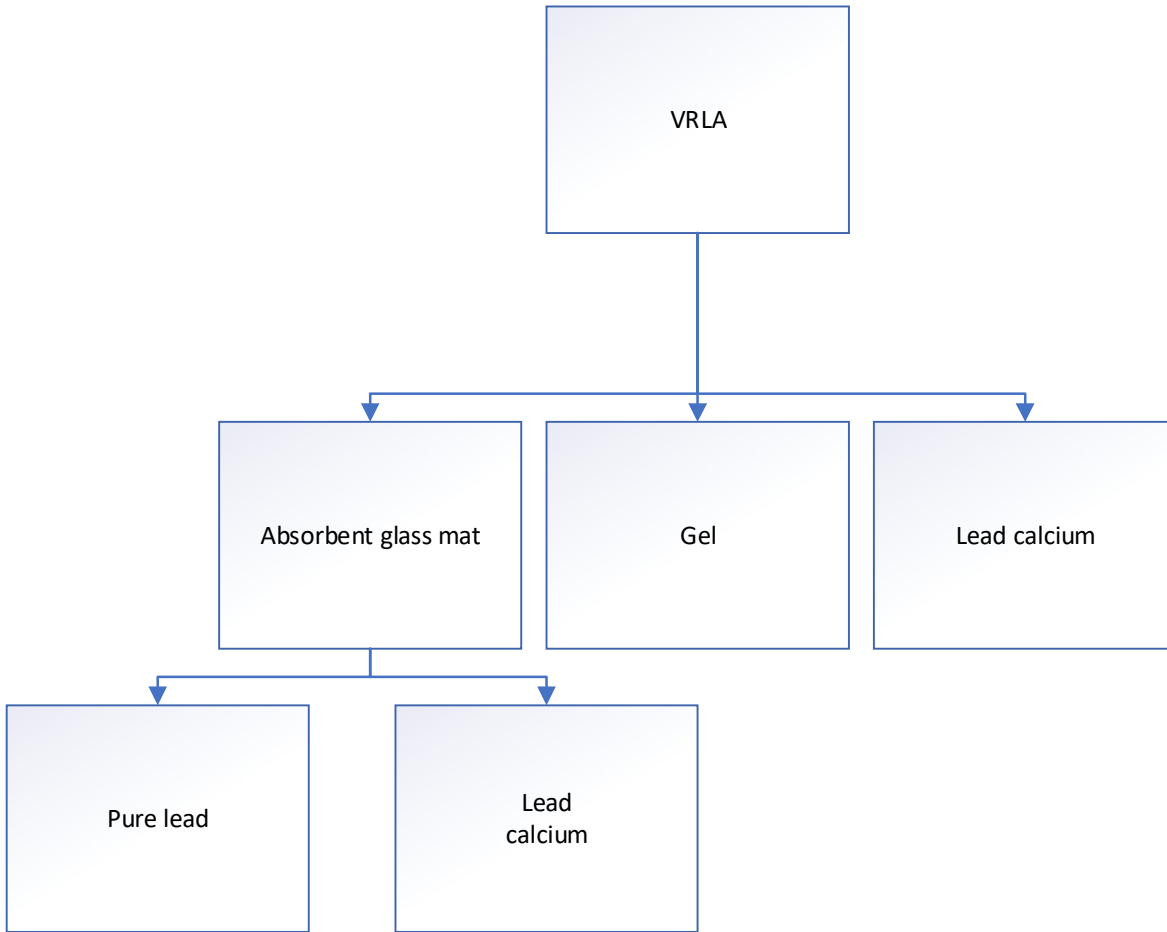


Figure 2.4 VRLA battery family

Table 2.2 Advantages of flooded cells

VLA	VLRA
Float current is lower	Lower Footprint
Longer life span (20 years)	Higher energy density
Better heat dissipation	Not spill able (lower maintenance/safer)

2.1.1 Alkaline Batteries

There are many different alkaline battery chemistries for standby applications, of which the most widely used one is Ni-Cd. They follow the basic battery structure with the anode consisting of a nickel oxide and the cathode being cadmium; the typical electrolyte is potassium hydroxide [21]. Being invented more than a hundred years ago it is a mature and well-studied

chemistry. The nominal voltage of a nickel-cadmium battery is 1.2 V. Some of the benefits of Ni-Cd batteries are their durability, good low-temperature performance, and ability to be charged at a high rate with little negative effects on the battery, combined with the fact that they can be stored at a discharged state and that they are not subject to special regulations when transported (they are not classified as a dangerous good) they are often used in mobile trailer applications [Figure 2.5].



Figure 2.5 Station (133 V) and communication (48 V) mobile trailer.³

On the other hand, Ni-Cd batteries suffer from high self-discharge, meaning that it hard to maintain them at a high SOC when stored; additionally they are not easily salvaged as cadmium is a toxic metal. They also require periodic full discharges in order to eliminate their memory effect [17] (i.e., their inability to hold charge).

2.1.2 Flow Batteries

Redox flow batteries are low efficiency but long cycle-life batteries. They operate by having an anolyte and catholyte at separate tanks while a pump moves the liquid to a common cell

³ Picture taken by Manitoba Hydro.

separated by a membrane. Of importance is that the only part requiring maintenance is the pumps (mechanical parts) and the technology is scalable and modular. The open circuit voltage per cell is between 1.2 and 1.3 V [22].

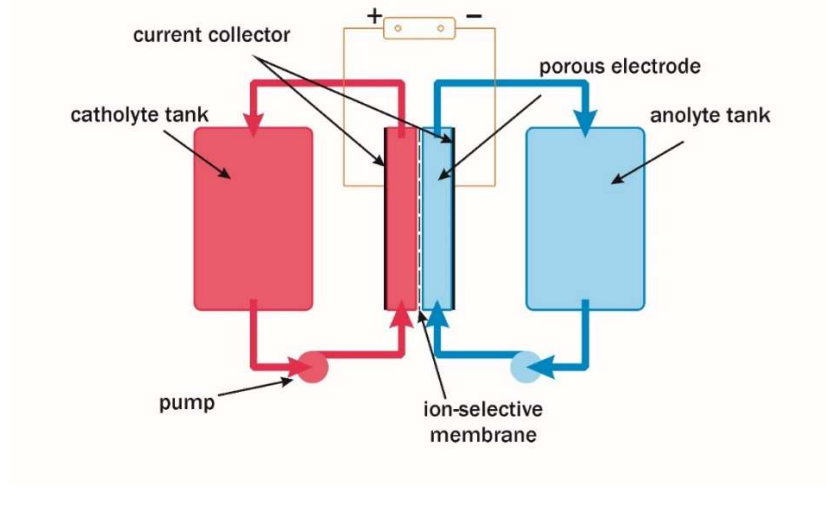


Figure 2.6 Flow batteries cell [35]

2.1.3 Chemistries Comparison

In Figures 2.7 and 2.8 different energy densities of various battery technologies are shown [23]. It is important to note that the information is generic and is at cell level and not at system level.

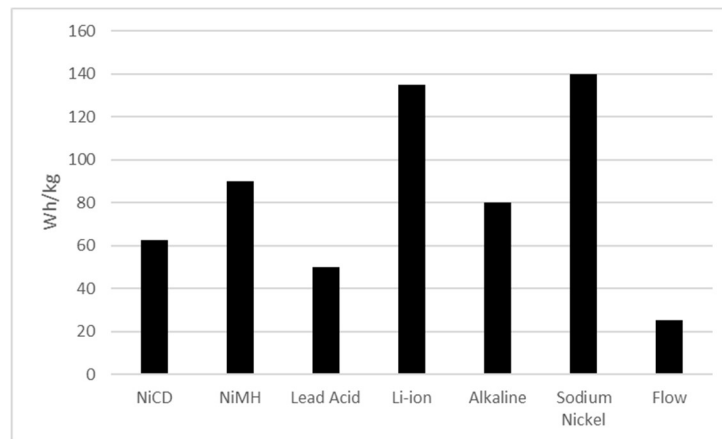


Figure 2.7 Energy density of different battery cells

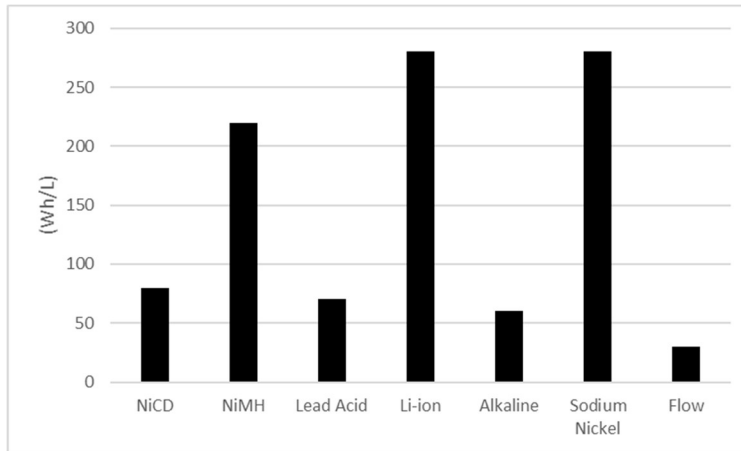


Figure 2.8 Specific energy of different battery cells

In a practical application what is important is the total footprint and the total weight (it is important to ensure that the floor can support the weight of the batteries). As an example, batteries that are able to stack on top of each other (as in the experimental setups of Chapters 3 and 4) provide the most energy in the least space. For a typical substation battery bank the comparison of size saving between lead-acid and lithium-ion/sodium-nickel chemistries is shown in Figure 2.9.

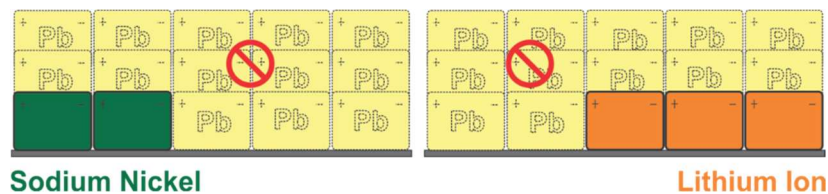


Figure 2.9 Lead-acid vs sodium-nickel and lithium-ion footprints.

2.2 Battery Models

The simplest possible battery model is an ideal voltage source (Figure 2.10). This would also describe an ideal battery, meaning that the discharge current and state of charge would have no effect on the voltage.

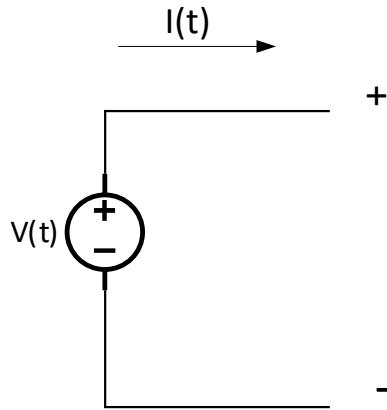


Figure 2.10 Ideal battery cell

The mathematic representation would be $V(t) = V$; the discharge curve of a 4 V cell using this model is shown in Figure 2.11.

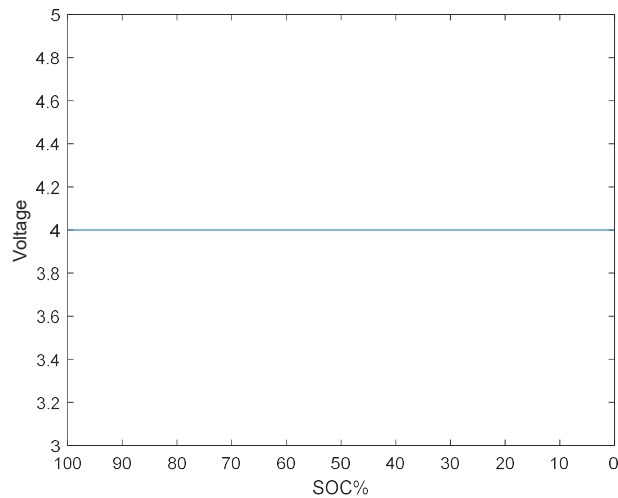


Figure 2.11 Ideal battery discharge

In reality a battery's voltage is dependent on its state of charge (SOC), meaning that a half-full battery will not be able to supply the same voltage as a full one. The relationship between

battery voltage and SOC is not linear and varies greatly between battery chemistries. Hence the first step into making a more accurate battery model would be to have values of voltage dependant on SOC, something that can only be done accurately experimentally. Battery voltage is also dependant on discharge rate hence it is important to note that the voltage we are interested in is the open circuit voltage (or rested voltage). A way to measure that voltage would be to discharge a battery cell to certain SOC values , let the cell rest and measure the voltage. Doing so would either be extremely time consuming or not very accurate depending on the number of measurements taken. An alternative faster and more accurate method would be to discharge the battery cell with a low discharge rate($C/20$ or more) which would emulate the open circuit voltage. For the purpose of this thesis a lithium-ion battery cell was connected to a constant load and was discharged at a rate of $C/25$ (Figure 2.12). These recorded values are essential in building a more accurate model.

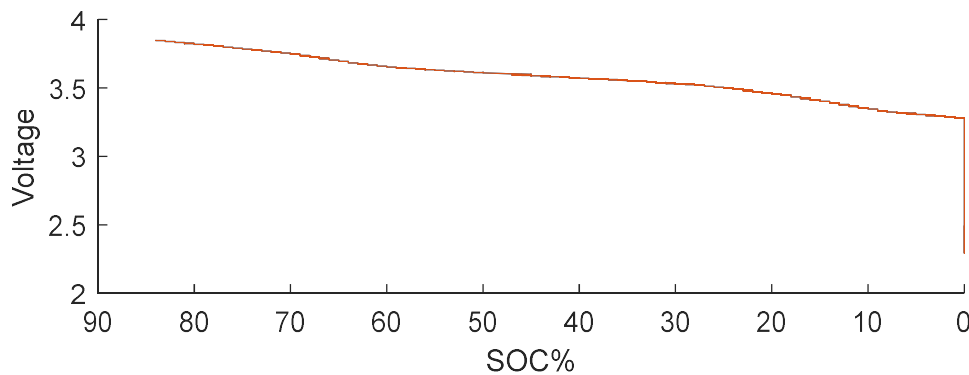


Figure 2.12 Open circuit voltage

As mention, a batteries voltage is also dependant on the discharge rate something that can be modelled by the addition of a series resistor to the SOC dependant voltage source. (Figure 2.13).

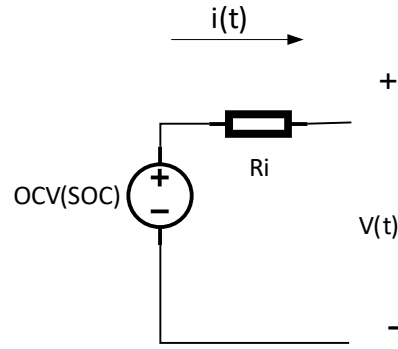


Figure 2.13 Resistance battery model

Mathematically the present model can be described as:

$$V(t) = OCV(SOC) - i(t) * Ri \quad (2.3)$$

Values for the resistance are often supplied by the battery manufactures but can also be calculated experimentally by the slope of the discharge. In the case of the battery cell tested earlier, no manufacturer data were available for the resistance hence the resistance was calculated experimentally (new lithium-ion cell) and was found to be 160 mΩ. The validity of this model can be seen in Figure 2.14 where a new lithium-ion cell was discharged at 90A and compared with the model based in Figure 2.13.

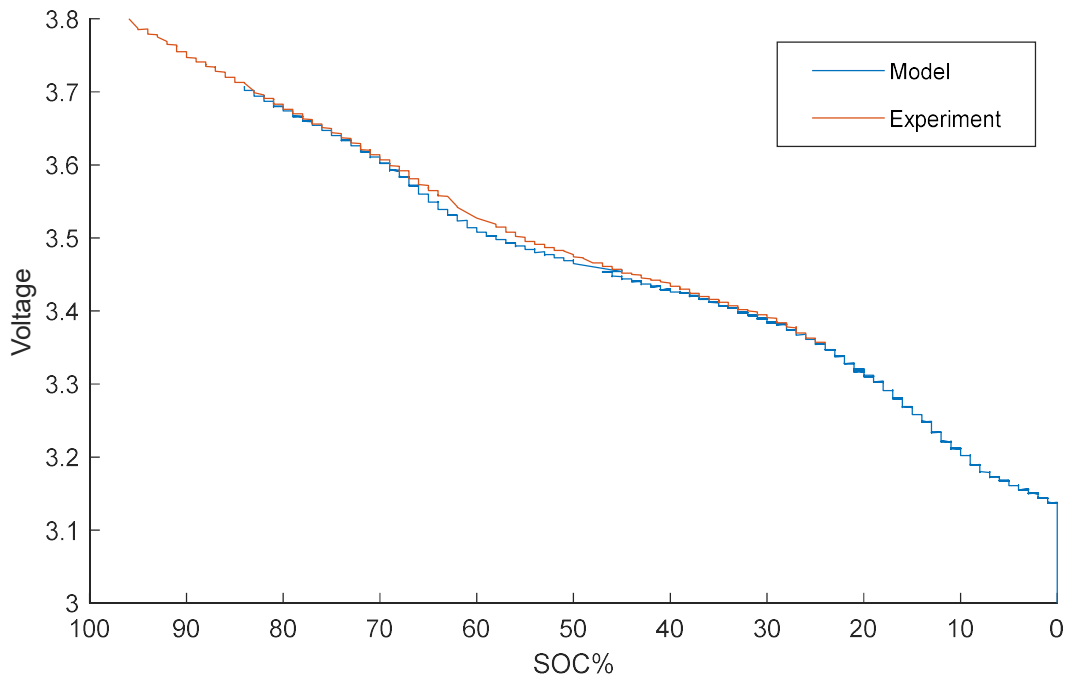


Figure 2.14 Experiment vs resistance battery model

While the model described in figure 2.13 is sufficient for stationary battery applications a more advanced model is worth discussing and it is one that can model the dynamic performance of a battery. This can be accomplished by adding an RC parallel branch [24] to the circuit (Figure 2.15), and is known as the Randall model.

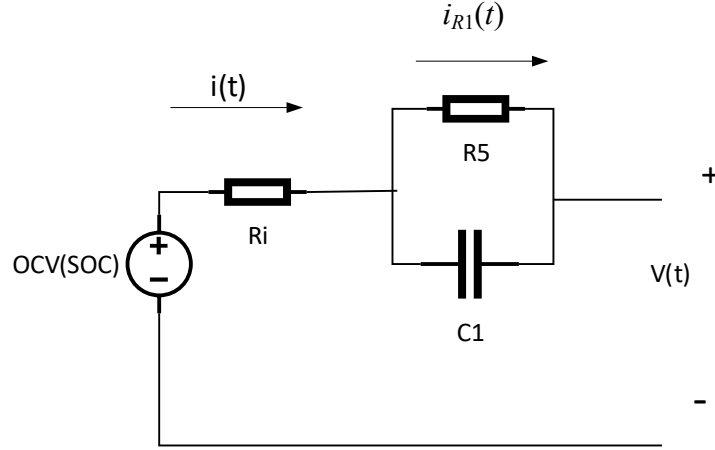


Figure 2.15 Randall battery circuit

The modelling expression would be as follows.

$$V(t) = OCV(soc) - i(t) * Ri - i_{R1}(t) * R1 \quad (2.5)$$

where $i_{R1}(t)$ would be the current across resistor $R1$.

The value of i_{R1} can be calculated by noting that

$$i(t) = i_{R1}(t) + C * R1 * \frac{di_{R1}(t)}{dt} \quad (2.6)$$

Solving for $i_{R1}(t)$ leads to

$$\frac{di_{R1}(t)}{dt} = -\frac{1}{R1 * C} i_{R1}(t) + \frac{1}{R1 * C} i(t) \quad (2.7)$$

This can be converted to discrete time ([24]), to be easily simulated in software, as follows.

$$i_{R1}[n + 1] = e^{\frac{-\Delta t}{R1 * C}} * i_{R1}[n] + (1 - e^{\frac{-\Delta t}{R1 * C}}) * i[n] \quad (2.8)$$

where Δt is the discrete time interval (usually the same value as the experimental sampling rate); it is assumed that $i_{R1}[0] = 0$. Values for R_1 and C can be only be extracted by analysing the experimental curves [24].

An alternative model not based on circuit theory is the Shepherd's model in which the voltage of a battery can be described as follows [25].

$$V = V_o - K \frac{Q}{Q - \int i(t) dt} i(t) - R_{in} * i(t) \quad (2.9)$$

where K is a polarization constant, Q is the battery capacity, $\int i(t) dt$ is the discharged capacity, $i(t)$ is the discharge current, and R_{in} is the internal resistance of the battery. V_o is equal to

$$V_o = K + R_{in} * i(t) + V(\text{steady state}) \quad (2.10)$$

$V(\text{steady state})$ is the voltage after the initial voltage drop caused by the discharge current. Shepherd's model accurately describes a batteries discharge as can be seen in figure 2.16, where a new lithium-ion battery cell is discharged at 90A is plotted against the models results.

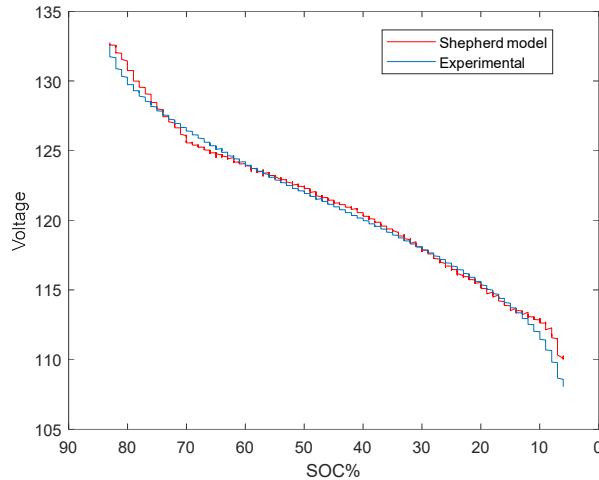


Figure 2.16 Shepherd model vs experimental data

2.3 Batteries in a Substation

The focus on this thesis is on stand-by batteries that are meant to be used in substations, a typical lead-acid substation bank can be seen in figure 2.17. Those batteries are designed to operate when normal power fails, and they are responsible for operating the station switches and breakers (Figure 2.18) as well as supplying a station's steady state load.



Figure 2.17 Substation battery bank⁴



Figure 2.18 Substation switchyard⁴

⁴ Picture taken by Manitoba Hydro.

Station standby battery banks are normally sized to provide sufficient power to the substation equipment over the entire substation duty cycle. The duty cycle used in two real Manitoba Hydro’s stations is shown in Table 2.3. Current magnitudes and the total duration of each section is determined based on following factors [26]:

- All steady state DC loads
- The worst-case protection events
- The DC loading for each switching device in the station
- Number of switching devices in the station

Table 2.3 Substation duty cycles

Section	66 kV station	115 kV station
A	266A for 1 min	67A for 1 min
B	8.1A for 239 min	16A for 239 min
C	120A for 5 min	30A for 12 min
D	8.1A for 234 min	16A for 227 min
E	128.1A for 1 min	46A for 1 min

A 66 kV station represents a typical distribution station while a 115 kV station does so for a transmission one. A distribution station has a lot more equipment hence the higher current needs. The durations for section A, B, and E are fixed and independent of the type or size of the station. Section C is calculated as the number of switching devices at a station divided by three. Finally, Section D is a station total duty cycle minus the duration of each other segment.

For current values, section A is calculated by considering the worst care protection event plus the steady state load (typical lights, ventilation heating/cooling of a station). Sections B and

D are the steady state load. Lastly sections C and E are depending on the type of switches devices and their needs.

It is important to note that this sizing information is based on IEEE and NERC guidelines and is meant for flooded batteries (mostly lead-acid). While there is continuous work towards their development, IEEE has not yet published technical guidelines that outline sizing standards for either lithium-ion or sodium-nickel battery systems. In Chapters 3 and 4 sizing procedures for lithium-ion and sodium-nickel batteries will be presented based on observations and experimental results obtained in this research work.

Chapter 3 Lithium-Ion Batteries

The first battery chemistry chosen to be experimentally tested was lithium ion. This chapter will start by explaining how lithium batteries work before moving on to experimental setups and results. Lithium-ion is one of the most researched and widespread battery technologies. The majority of energy storage applications installed yearly have been based upon lithium-ion [27]. In addition, it is the battery of choice for most electric vehicles as well as consumer electronics. On the other hand, its implementation in substation application is not as widespread. The purpose of this chapter is to offer a generic introduction to lithium-ion battery technology and give the results and experiences from nearly two years of using this chemistry in a previously untested environment.

A common misconception about lithium-ion batteries is that they are all considered the same. However, when dealing with lithium-ion batteries one should instead be treating them as a large family where each member may vary greatly. As it is evident by their name all lithium-ion chemistries consist of lithium-ion atoms. The lithium-ions carry electrons between a positive and negative electrode (Figure 3.1). In literature the positive electrode is often referred to as a cathode and the negative as an anode; however, those terms would only be accurate while a battery discharges and will be reversed while the battery charges. The positive electrode of a lithium-ion battery consists of either phosphate (e.g., LFP) or metal-oxides (e.g., NCA) [27]. The negative electrode can be either carbon (most of the time Graphite) or lithium-titanite. Both the electrodes are within an electrolyte (it can be aqueous or not) that allows the movement of electrons. The last component would be a separator that separates the positive and negative sides.

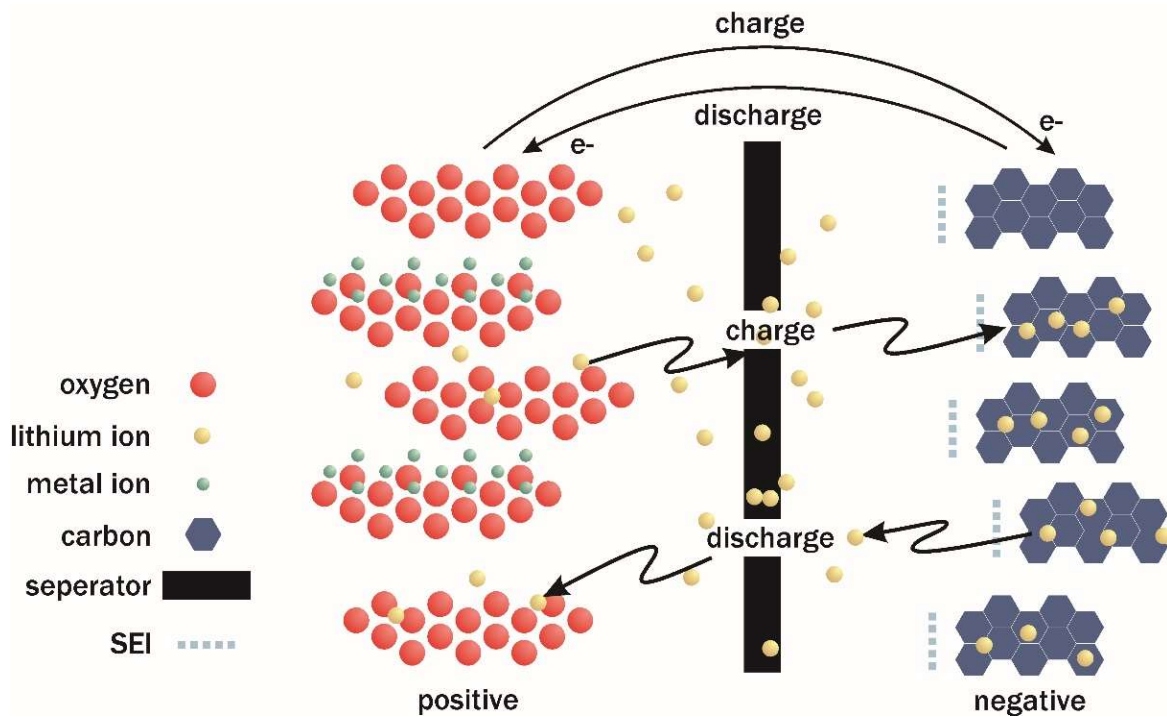


Figure 3.1 Lithium-ion cell reactions [27]

Depending on the choice of positive and negative components the characteristics of a lithium-ion battery can vary greatly. There are implementations that offer very high voltages per cell (more than 4.5 V), but offer reduced capacity, or vice versa. When choosing a lithium-ion battery it is important to understand the positive and the negatives of each chemistry and choose the right chemistry for the right application; for example, a lithium-ion battery meant for a phone or a laptop would require high cycle count potential while in a battery meant for a substation one would look for an increased calendar life.

3.1 Experimental Setup for Calendar Aging

The first installation was commissioned in the summer of 2016 at a Manitoba Hydro training centre, where they were connected to a mock substation that includes hydraulic solenoid circuit breakers and Motorized Operating Disconnects (MODs), which operate frequently for training purposes. The location was chosen as it would allow frequent cycling and usage of the batteries in their intended application. The size of the battery bank was chosen to be 180 Ah plus 90 Ah of redundancy. This battery banks size would be suitable for a small to medium size substation. The system (Figure 3.2) consisted of three parallel strings each with a 90 Ah capacity. There were five 24 V modules (Figure 3.2) in series in each string.



Figure 3.2 Stonewell experimental setup

Initially the batteries were charged to 129 V (station voltage), which corresponded to them being kept at 85% SOC. The batteries were kept on float except for when they underwent occasional capacity tests or were discharged in order to activate the station interrupting apparatus.

Roughly nine months after installation, the battery potential was increased to 140 V (representing 100% SOC) in order to investigate how typical station equipment would respond to the higher voltage ensuing from an emulated BMS failure. The Battery Management Module (BMM) of the batteries allowed a PC connection and use of diagnostic software to record various battery parameters (e.g., minimum/maximum cell voltage).

As an initial test the values for the instantaneous resistance were calculated after performing a Current-Off Test as discussed in [34], using the current discharge profile shown in Figure 3.3 and measuring the voltage change caused by said discharge (Figure 3.4).

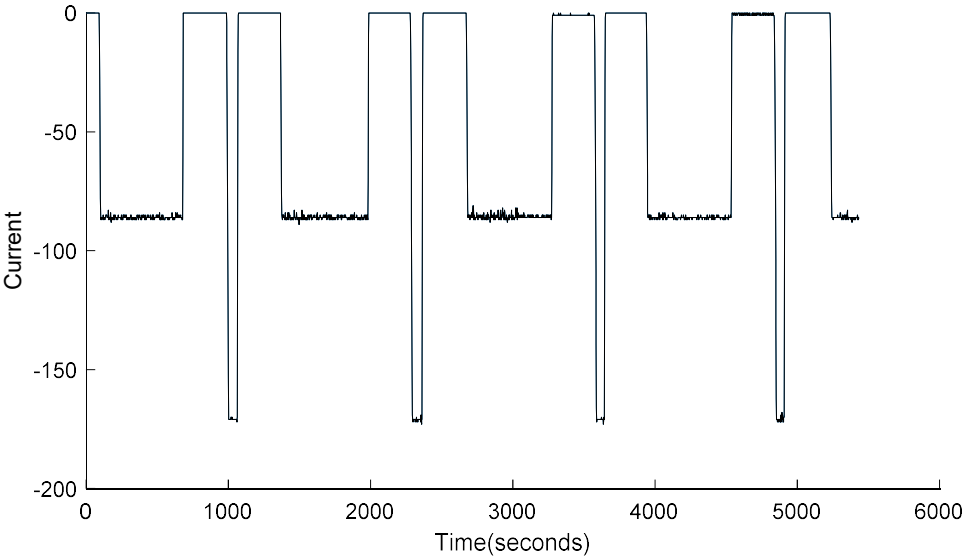


Figure 3.3 Current-off discharge profile

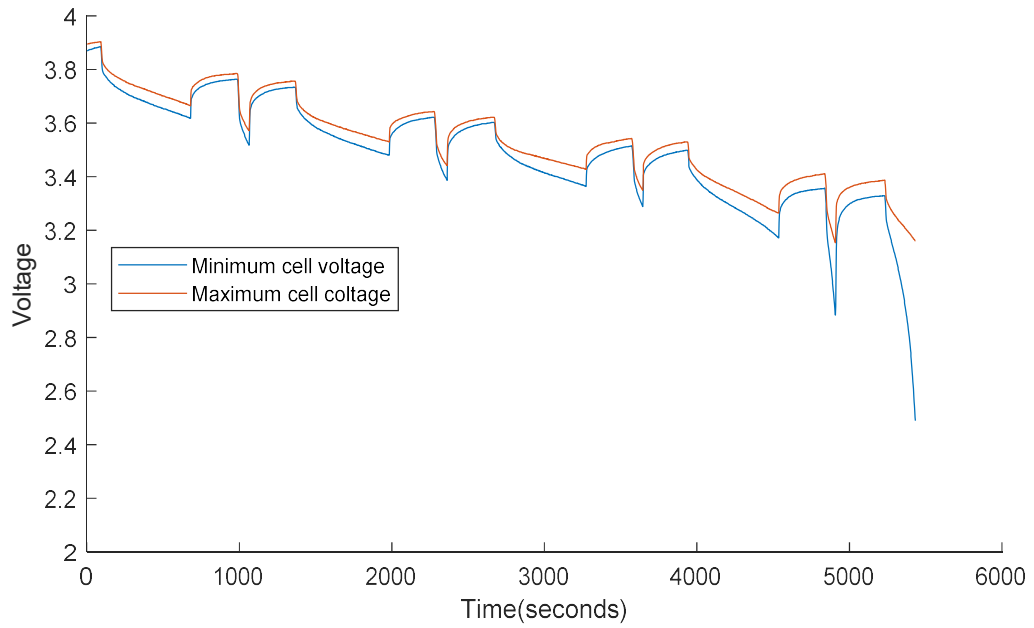


Figure 3.4 Cell voltage during current-off test

Although the current-off method is not the most accurate it is adequate as a comparison tool and was chosen for its simplicity. Table 3.1 shows a comparison between the instantaneous internal resistances of a new battery against a calendar aged 18-month-old battery.

Table 3.1 Instantaneous resistance calculated 18 months apart

Depth of discharge	New batteries R (m Ω)	18-month batteries R (m Ω)
27%	0.68	0.90
31%	0.62	0.76
49%	0.53	0.75
53%	0.64	0.86
69%	0.36	0.75
73%	0.54	0.85
89%	0.76	1.93
93%	0.86	N/A

Even when factoring in calculation errors from the methodology, and test procedure variations, there is a noticeable increase in internal resistance after 18 months, and particularly on higher DOD. It is vital to note that the 18-month batteries were unable to fully complete the discharge profile of Figure 3.3 (reached terminal voltage before the duty cycle concluded). It is also important to note that batteries installed in the field will be discharged far less frequently if at all, in comparison to those discussed in this chapter, hence the increase of the internal resistance is likely to be lower.

In addition to the current-off tests, of even greater importance are the capacity tests results. Figure 3.5 compares a new battery's cell voltage to that of an 18-month old battery when both are discharged at 1C (90 A). The batteries lost between 4.4% to 6.6% of their rated 90 Ah capacity over this 18-month period (Table 3.2).

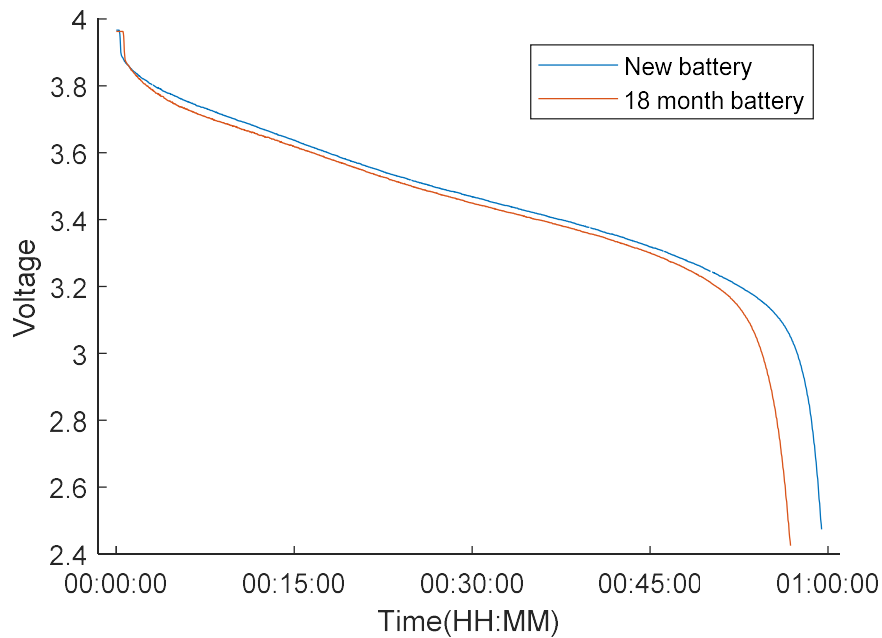


Figure 3.5 1C discharge of new and aged batteries

Table 3.2 Calendar aged lithium-ion batteries

Battery string rated 90 Ah	Capacity (Ah)	Capacity loss (%)
String 1	85	5.50
String 2	86	4.40
String 3	84	6.60

3.2 Accelerated Aging Tests

In December of 2017 two additional lithium-ion systems were commissioned for experimentation and testing purposes. Four strings of three 24 V modules were each mounted on a rack and placed inside an oven (Figure 3.7). The string battery management systems were placed outside the oven to protect the electronics, and to allow for easy connection of the diagnostic tools (Figures 3.8 and 3.9). It is important to note that cell management is done by electronics inside each individual module and, therefore, are subjected to increased temperature of the oven. It is expected that exposing the batteries to oven temperatures would accelerate the battery aging process [28]. The oven was set at 60°C, which is the maximum temperature recommended by the manufacturer. Storage at higher temperatures would lead to additional chemical reactions inside the battery cell that do not correspond to those that occur under normal operations [29]. The temperature of the modules was monitored with both the BMS diagnostic software and a FLIR infrared camera and there were no large deviations in temperature between modules (< 2°C).

Each string was stored at a different SOC. Module 1 at 20%, Module 2 at 50%, Module 3 at 80%, and Module 4 at 100% connected to float.



Figure 3.6 Battery strings inside oven



Figure 3.7 BMS setup



Figure 3.8 Oven-charger-BMS setup

The current-off method was again used for the determination of the internal resistance. A different discharge profile (Figure 3.10) was used (compared to Figure 3.3) tailored to the reduced voltage of a 3-module system (83 V). As seen in Figure 3.11 this discharge profile does not allow rest time for the batteries leading to a faster drop of voltage that would more accurately describe real station conditions.

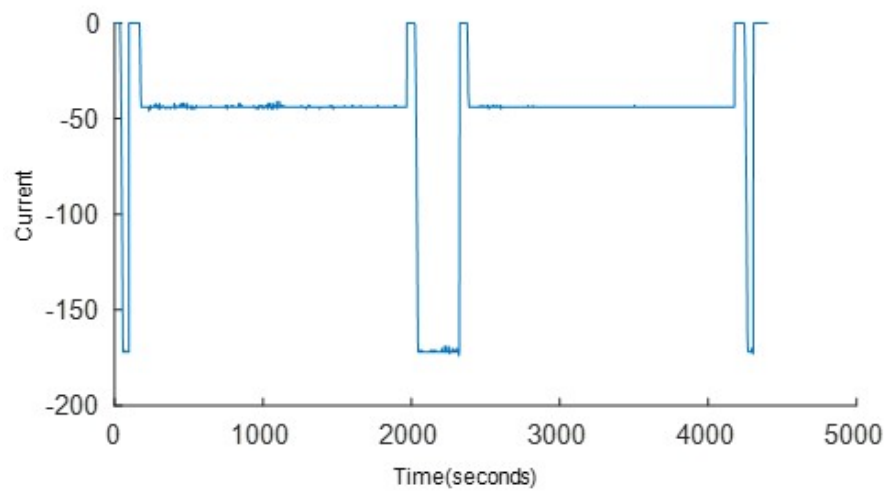


Figure 3.9 Discharge profile for the 83 V system

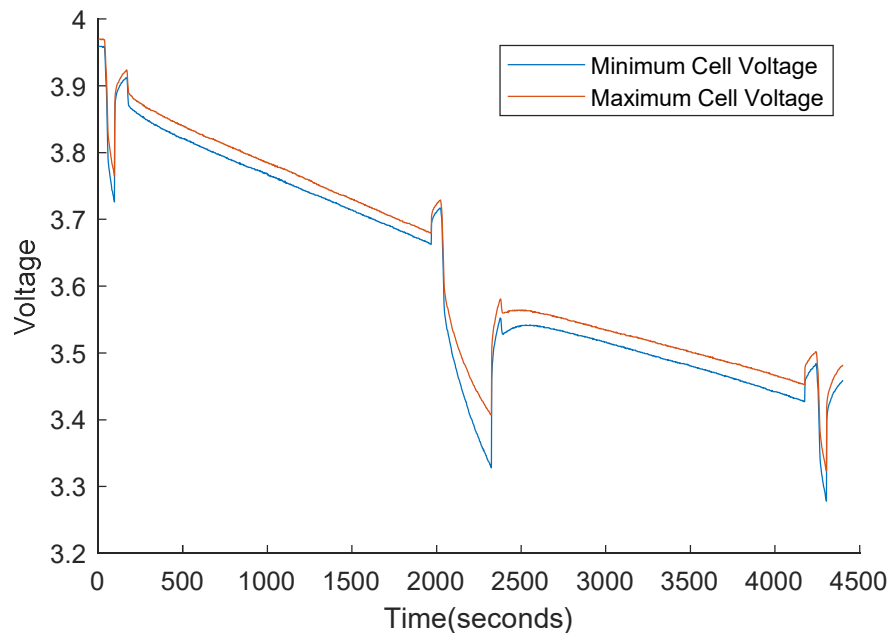


Figure 3.10 Cell voltage of the 83 V system (new batteries)

Table 3.3 shows the measured internal resistances of the batteries after being stored at 60°C for two months. The initial results have shown that batteries stored at a lower SOC have a lower internal resistance. Further measurement will be taken to determine if the trend continues although results seem to agree with those obtained by M. Lewerenz [30].

Table 3.3 Batteries stored at 60° Celsius

Depth of discharge	R (m Ω)			
	20% SOC	50% SOC	80% SOC	100% SOC
2%	0.46	0.49	0.68	0.6
30%	0.48	0.69	N/A ⁵	0.71
40%	0.63	0.67	0.72	0.65
54%	0.44	0.47	0.67	0.69
59%	0.47	0.51	0.66	0.64

⁵ Value could not be calculated due to failure on recording equipment .

Although performing pulse tests and measuring internal resistances is expected to be of future use in statistical modelling, what is also of interest is how batteries perform on a duty cycle of a real substation. Due to time constraints an accelerated and more intense duty cycle was used (Figure 3.12), over the one normally used in the field.

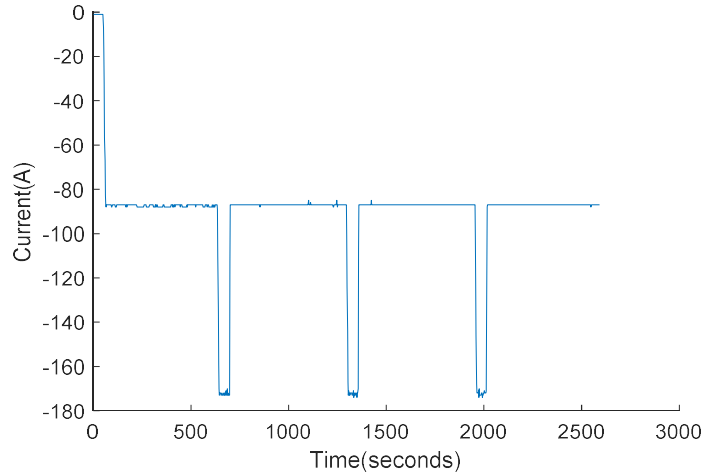


Figure 3.11 Intense discharge current

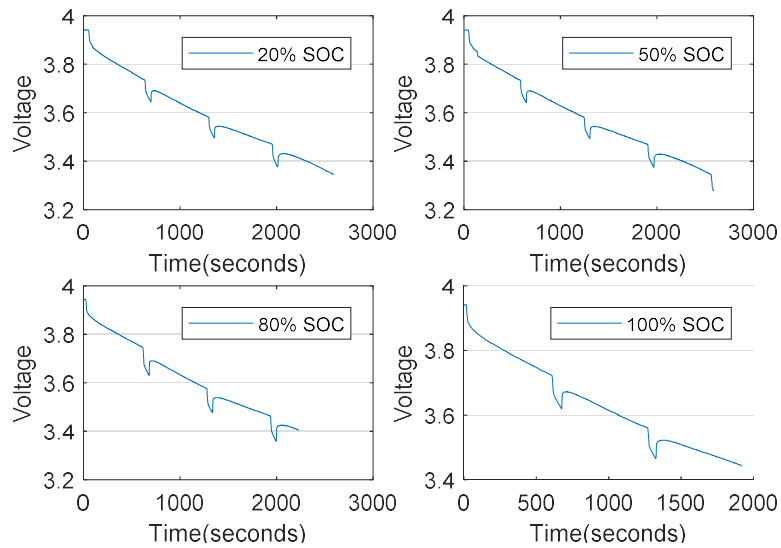


Figure 3.12 Minimum cell voltage for batteries stored at 60°C

As it is expected from the internal resistance discrepancies, the systems performed differently and there are clear differences in the discharge ability of each string (Figure 3.13). The systems stored at a lower SOC (20% and 50%) were able to discharge 67 Ah and 69 Ah before critical voltage. On the other hand, the systems stored at 80% and 100 % were only able to discharge 56 Ah and 48 Ah, respectively.

Figures 3.14 and 3.15 show the results of the capacity tests performed at 1C. The batteries that were stored at a lower SOC were able to discharge for longer periods. As it can be seen in Table 3.5 in only 6 months there was an almost 9% variance between the highest and lowest performers.

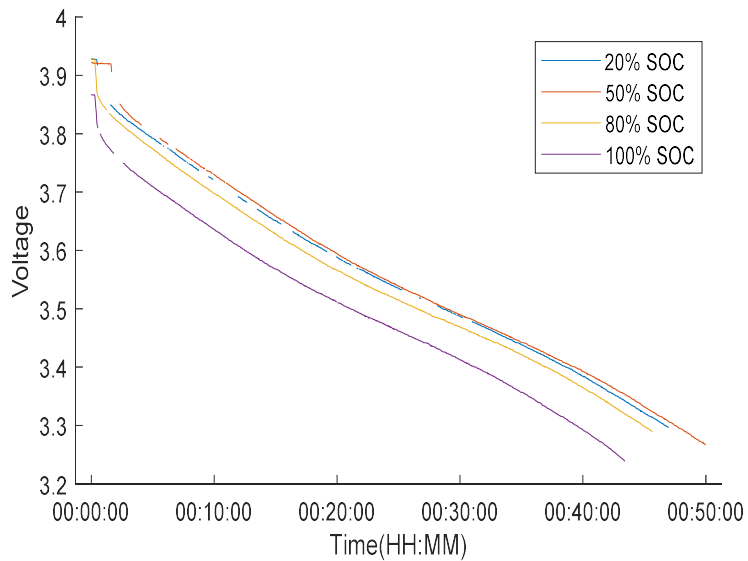


Figure 3.13 1C discharged batteries stored at 60°C.

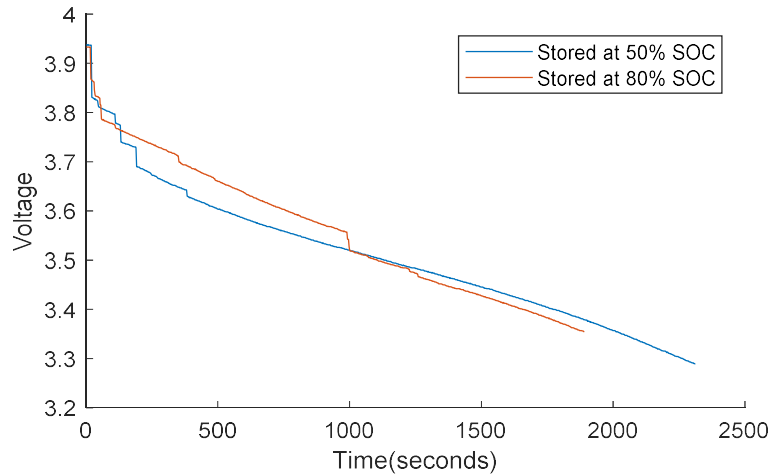


Figure 3.14 1C discharge of batteries stored at 60°C

Table 3.4 Accelerated aged lithium-ion batteries

Battery string rated 90 Ah	Capacity (Ah)	Capacity loss (%)
20% SOC	69	23.3
50% SOC	72	20
80% SOC	67	25.5

3.3 Summary and Sizing

The batteries stored at 50% SOC exhibited the best performance, suggesting that battery life can be extended by oversizing the battery bank and floating it at a lower SOC. However, conservatively assuming that lithium-ion capacity degradation continues at a compounded 4% annual linear rate, a battery bank must initially be significantly oversized to have sufficient capacity over a 20-year period. For instance, supplying a 180 Ah station load for 20 years would require initially sizing the bank to 400 Ah. Alternatively, because the BMS enables simultaneous operation of multiple capacity modules, additional modules could instead be added at fixed intervals. For example, the initial bank could initially be oversized by 90 Ah and then new 45 Ah

modules could be added every 5 years to account for degradation. This approach suffers from the drawback of requiring increased labour and maintenance, which obviates the original rationale for installing such technologies. Although lithium-ion battery experimentation continues, these results are among many factors that led to the conclusion that this technology is not yet suitable for dependable cost-effective adoption within substations.

Since the tests performed were very experimental and in unique conditions there were several incidents that were unexpected. One of the major ones was observed in the four-string implementation where significant back charging between strings were recorded, with charging currents in excess of 70 A for an individual string.

Considering the charging of the cells is limited to 40 A a charge current of almost double that can have a major effect on the longevity of the cells and can be a safety concern. In addition, while the presence of BMs help control the batteries, it was noticed that if the batteries were discharged below a certain voltage, the BMS would not allow the batteries to charge (as there is not enough power to power the BMS). The solution to that was to bypass the BMS entirely and directly connect the cells to the charger.

Chapter 4 Sodium-Nickel-Chloride Batteries

The second technology tested was a sodium-nickel-chloride battery. Sodium batteries were first originated during World War II with the purpose of being used in rockets. Sodium-nickel-chloride technology is also claimed to have been invented in south Africa and it was nicknamed Zebra battery [22]. Currently there is only one manufacturer of sodium-nickel-chloride battery (FZsonick).

When manufactured the active materials of the batteries are sodium chloride and metal powders (majority of it being nickel). After the battery is charged, they change to sodium and metal chlorides [31].



The electrolyte is Beta-Alumina (β "alumina) while the battery is in a cool state and NaAlCl_4 while the battery is in operation. In Figure 4.1 a sodium-nickel-chloride battery cell can be seen while Figure 4.2 shows its internal components. (pictures are used with permission from FZsonick). The open circuit voltage of each cell is 2.58 V and the capacity is 40 Ah.



Figure 4.1 Sodium-nickel-chloride cell

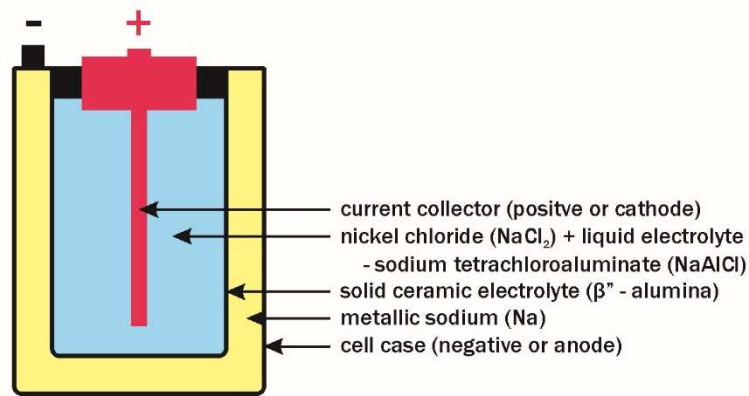


Figure 4.2 Representation of sodium-nickel-chloride internal components

Sodium-nickel-chloride batteries contain an internal BMS and a 100W (at 20°C ambient temperature) heating element that maintains their operating temperature, which varies the batteries' internal resistance and therefore their capacities. When “cool,” sodium-nickel batteries have almost infinite internal resistance and can, therefore, be treated as an open circuit. To reach minimum internal resistance and hence maximum capacity, the battery must run for at least 15 hours to reach a 265°C operating temperature.

4.1 Experimental Setup

Due to their high energy density the batteries were chosen to be tested as a substation battery. To the best of the author's knowledge this was the first time that this chemistry was tested under this condition.

The testing system consists of two modules rated at 110 V with an 80 Ah capacity. Their float voltage was set at 130 V with rest voltage being at 117 V. This was lower than the desired substation voltage (133 V) but at the time of purchase there was no option available for the desired substation voltage.



Figure 4.3 Stonewell sodium-nickel-chloride experimental setup

Float voltage works differently in sodium-nickel-chloride batteries in comparison with other chemistries. These batteries can be kept on float on a much higher voltage than their rated, as a converter is used to change it to the desired. Furthermore, the batteries do not self-discharge, hence no charge “top up” is needed. When the battery is fully charged the float voltage is only used to power the internal heater of the batteries.

The sodium-nickel-chloride batteries’ capacity was experimentally found to depend on their current discharge rate, with $C/4$ rates providing the largest capacity. Reducing discharge rates to below $C/4$ diminishes the battery capacity due to the power consumption of the internal heating element and BMS (roughly 100W). Discharges over $C/4$ increase the internal temperatures of the battery to critical levels prompting the BMS to shut down the system in order to protect the batteries. This can be seen in Table 4.1 where the test terminated while the batteries still had power available (SOC remaining).

Table 4.1 Sodium-nickel-chloride capacities

Discharge rate	Rated capacity	Measured capacity	Capacity discrepancy	Test duration	SOC remaining at test conclusion
C (80 A)	60.0 Ah	51.0 Ah	15%	39:05 min.	43.50%
C/2 (40 A)	76.4 Ah	70.0 Ah	8.4%	105:00 min.	7.00%
C/4 (80 A)	80 Ah	79 Ah	1.25%	Not recorded	Not recorded

Although test results deviated from manufacturer specifications when the batteries were discharged at current rates that exceeded C/4, no capacity loss in the batteries themselves was detected over the first 18 months of operation.

Testing currents were limited to 125 A because of the system’s internal circuit breaker. The most significant concern with sodium-nickel-chloride batteries was whether a high current would cause the internal temperature to reach critical values and thus shut down the battery. With the tests performed this was achieved using a current of 110 A for less than 30 min. Two different load profiles were tested. These profiles are shown in Figures 4.4 and 4.5.

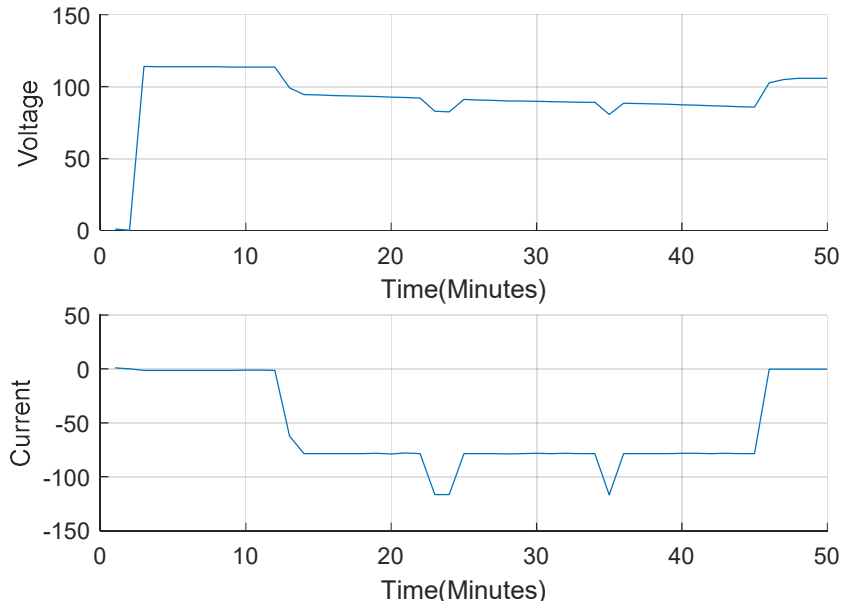


Figure 4.4 Voltage (top) and Current Discharge Profile (bottom)

In the case shown in Figure 4.4 the voltage dropped from 114 V to 79.6 V at the end of the test after discharging a capacity of 45 Ah.

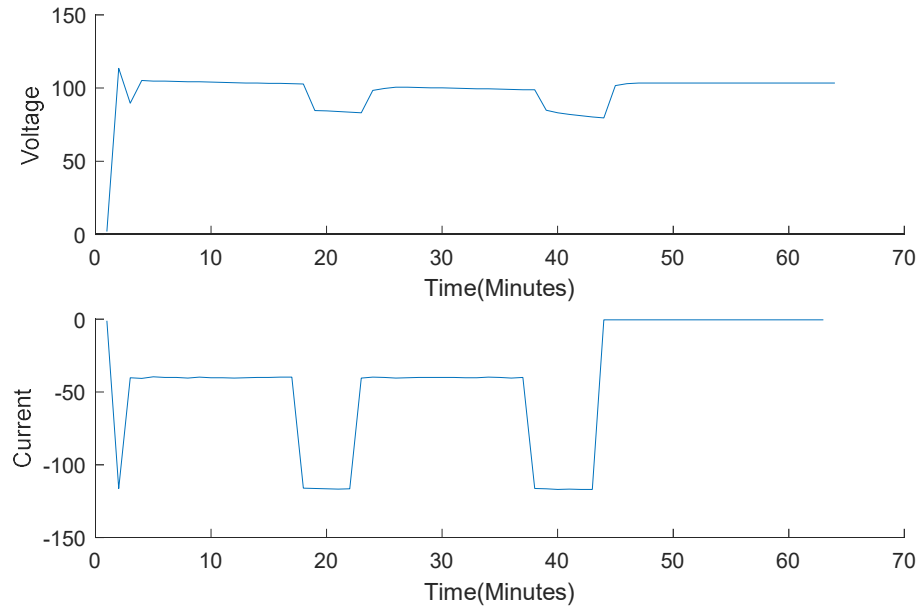


Figure 4.5 Voltage (top) and Current Discharge Profile (bottom)

In the case in Figure 4.5 the voltage dropped from 114 V to 85.7 V at the end of the test discharging 43.5 Ah. In both cases the BMM terminated the test. The internal temperatures of 340°C were very close to the disconnect point of 350°C. Of importance is that there was no significant drop in voltage through various SOCs. In addition, the internal resistance remained stable when the battery was discharged at rates below $C/2$.

4.2 Implementing Sizing Practices

Since the technology has never been tested in the current application there are no sizing standards for those batteries. As the battery capacity is dependent on their discharge rate the first step to developing sizing practices would be to calculate the capacity for different discharge rates.

Table 4.2 Capacity for different discharge rates

Discharge rate	Discharge rate (decimal)	Capacity (Ah)
C	1.00C	51
C/2	0.50C	70
C/4	0.25C	79
C/6	0.17C	78
C/8	0.13C	77
C/10	0.10C	75
C/15	0.07C	69

When the battery discharges at lower rates the internal heater supplies some of the energy, and hence the reduced capacity. The next step would be to calculate the total capacity requirement based on a station's duty cycle; this offers a rough estimate of the amount of batteries that are to be used.

Table 4.3 Duty cycle example 66 kV station

Section	Current (A)	Duration (min)	Capacity used (Ah)
A	266	1	4.40
B	8.10	239	32.2
C	120	5	10.0
D	8.10	234	31.6
E	128.1	1	2.14
Total		480	80.3

Based on the calculations performed a battery capacity of 80.34 Ah would be enough for the station needs. However, sodium-nickel-chloride batteries only come in 80 Ah modules, hence at least two modules must be used. Since the internal breaker of the battery is rated at 125 A two modules would not be able to supply the stations load. Hence for the station in question, three modules will have to be used. Most of the duty cycle is spent on the steady state operation of the

station (areas B and D) hence optimally those discharge currents should be as close to C/4 of the battery capacity as possible. In this case areas B and D are close to C/30, which can be estimated to a capacity of 54 Ah per module (assuming linear discharge and 100 W heater usage).

It is possible to estimate the capacity needs by assuming a fixed capacity based on the discharge rates of the longest event; in the case of the discharge in Table 4.3, the total capacity of the battery would then be 162 Ah, which would be enough to cover the 80.34 Ah needs.

While this method may be enough for oversized banks a more accurate method will have to be developed. This can be accomplished by scaling the capacity based on the discharge rate for each section.

As an example, a rated 240 Ah battery bank will have a 147 Ah capacity when discharged at 1.1C. The Ah requirements of the section would then be subtracted. Finally, the new capacity will be scaled according to the next discharge rate capacity. Shown in Table 4.4 are the results of this sizing method for a 66 kV station.

Table 4.4 66 kV station sizing example

Section	Needed capacity (Ah)	Discharge current (A)	Discharge rate	Discharge rate ⁶ capacity (Ah)	Scaled capacity (Ah)	Remaining capacity (Ah)
A	4.4	266	1.1 C	147(49)	147.0	143.0
B	32.2	8.1	0.03 C	162(54)	157.1	124.9
C	10	120	0.5 C	210(70)	161.9	151.9
D	31.6	8.1	0.03 C	162(54)	117.0	85.60
E	2.14	128.1	0.53 C	216(72)	114.0	111.9
Total	80.34				Scale to rated 124	

⁶ Parenthesis indicate the per module capacity

A similar procedure can be used for the 115 kV station (Table 4.5). The Ah needs of this station are higher than those of the 66 kV station; however, due to the lower current demands two 80 Ah modules may be enough to supply it. As shown from Table 4.6 that is indeed the case.

Table 4.5 Duty Cycle example

Section	Current (A)	Duration (min)	Capacity used (Ah)
A	67	1	1.10
B	16	239	63.7
C	30	12	6.00
D	16	227	60.5
E	46	1	0.77
Total		480	132.1

Table 4.6 115 kV station sizing example

Section	Needed capacity (Ah)	Discharge current (A)	Discharge rate	Discharge rate ⁷ capacity (Ah)	Scaled capacity (Ah)	Remaining capacity (Ah)
A	1.10	67A	0.280 C	158(79)	158.0	156.9
B	63.7	16A	0.060 C	138(69)	137.0	73.33
C	6.00	30A	0.125 C	156(78)	82.90	76.90
D	60.5	16A	0.060 C	138(69)	68.00	7.530
E	0.77	46A	0.190 C	158(79)	8.620	7.850
Total	132.1				Scale to rated 9.9	

⁷ Parenthesis indicate the per module capacity

In summary sizing of sodium-nickel-chloride batteries can be described by the following steps.

- 1) Calculate the station's Ah capacity needs
- 2) Estimate the number of modules needed to supply this Ah at rated capacity
- 3) Check current needs making sure the batteries would be able to supply it (depends on breaker rating)
- 4) Estimate battery capacity based on longest discharge (Approximation for cost estimation and planning)
- 5) Compare the capacity to the demand
- 6) Perform detailed analysis based on each discharge rate
- 7) Compare the capacity to the demand

4.3 Developing Maintenance Guidelines

Experimental results suggest that the sodium-nickel-chloride batteries tested are capable of not only meeting the needs of the utility in the specialized applications for which they were initially envisioned but also being competitive with VLA batteries in conventional substation standby and communications applications. However, before a utility can use them there is a need to integrate these batteries into its existing asset management program, which encompasses estimating the purchase, commissioning, lifetime maintenance, and retirement costs of employing this technology, along with determining prudent spare component levels and developing initial Asset Health Index parameters to quantify the battery, charger, and BMS conditions and track their degradation over time.

An initial Reliability-Centred Maintenance (RCM) analysis of the sodium-nickel-chloride batteries is performed before including the assets into a maintenance program. RCM analysis provides a structured framework that analyses an asset's functions and failures to develop an efficient maintenance plan that balances cost-effectiveness against acceptable levels of risk and operability.

A well-functioning RCM program enables a utility to reduce and eliminate chronic failures and reliability problems, reduce unscheduled maintenance (which is typically estimated to cost roughly ten times more than planned maintenance), document practices, and prioritize actions based on equipment criticality. A structured methodology for capturing performance data provides sufficient confidence in the data to optimize an asset's performance based upon availability, downtime, and maintenance costs information.

Optimizing the task selections and intervals requires a continuous improvement phase and a control phase, which first monitors for opportunities and then successfully implements the change. Including severity of failures for task selection criteria can facilitate analysis by focusing on task selections that address forced and functional failures. Traditional RCM theory requires answering the following seven essential questions [32]:

- 1) What is the function of the asset?
- 2) What can cause it to fail to function?
- 3) What causes those failures?
- 4) What happens when there is a failure?
- 5) How important is each failure?
- 6) How can failures be prevented?
- 7) What is the default action?

This thesis simplifies the process somewhat by employing a streamlined version of RCM for the sodium-nickel-chloride batteries. This streamlined component-based RCM program is based on discovering all the possible ways a device can fail (“failure modes”), the reasons for which they fail (“failure causes”) and the most effective tasks to detect their impending failure (“task selections”). This is collectively referred to as “Mode/Cause/Task” (M/C/T) analysis. Despite its relative simplicity, this remains an involved process that first requires undertaking a detailed study of all an apparatus’ component and subcomponent systems in order to anticipate the failure modes. A thorough knowledge of diagnostic equipment and tests is next required in order to understand the abilities and limitations of the data collection needed to uncover such failure modes.

Upon identifying all possible failure modes, the causes of each failure and the most cost-effective task to identify and mitigate each cause of failure is determined (Table 4.7). Maintenance tasks are divided into routine and non-routine tasks (Table 4.8). In this case, the dc system has been divided into its three major constituent components, comprising the battery, its charger, and the battery management system (BMS).

Table 4.7 Mode cause task

Component	Failure Mode	Causes	Most effective task
Battery	<u>Battery is inoperable</u>	Battery Main Circuit Breaker Open	Functional Test
		Fault in the Main Contactor	Functional Test
		String Voltage Unbalanced	Functional Test
		Temperature Probe Error	Functional Test
		Battery Controller Failure	Functional Test
		Battery Smoke Detected	Functional Test
	<u>Disconnected from Bus</u>	High BMS temperature	Integrity Check
		Low voltage on DC Bus	Functional Test
		High Voltage on DC bus	Functional Test
		Battery Voltage low	Integrity Check
		Battery Voltage high	Functional Test
		High discharge current.	Functional Test
		High charge current	Functional Test
		Low BMS temperature	Integrity Check
		Heating System Fault	Functional Test
		High Battery Cell temperature	Functional Test
	<u>Failure to Provide Rated Capacity</u>	Cell damaged	Functional Test
		High Temperature	Functional Test
		Low Temperature	Integrity Check
Under charged		Integrity Check	
Over charged		Functional Test	
Over discharged		Functional Test	
<u>Failure to Conduct</u>	Grounds	Integrity Check	
	Loose connections	Integrity Check	
Charger	<u>Failure to Provide Rated Capacity</u>	Loss of regulation	Functional Test
		Loose Connections	Integrity Check
BMS	<u>Unable to display alarms</u>	Loose connection	Integrity Check
		BMS damaged	Functional Test

Routine tasks were further divided into integrity and functional tests. Integrity checks are intended to be performed while the apparatus remains in service. Functional tests require more time and require removing the equipment from service. As no historic data exists for the first year of operation. Periodic firmware upgrades are expected to be needed in order to deal with future software compatibility issues, between the BMS and the maintenance equipment.

Table 4.8 Maintenance tasks

Routine maintenance tasks		Non-routine maintenance tasks
Integrity check	Functional test	
Visual inspections	BMS functionality/PCB test	Transportation
Verify connections	Externally measure and verify battery temperature via BMS	Installation & Commissioning
Check room temperature	Float current of batteries/charger	Capacity tests
Check room condition	Discharge history	Firmware upgrades
Verify safety equipment is present and operational	Measure and verify float voltage	Salvage and disposal
Test BMS alarms	Download discharge history and battery data	

Because these batteries are newly introduced, and little reference material exists, both functional and integrity checks will be performed immediately after each battery discharge, or every six months if they do not discharge. This will continue for the first 24 months following commissioning. The maintenance intervals will then be modified using the data collected in conjunction with Bayes' Theorem, with a 90% reliability rate targeted and with the prior being determined by the batteries' aggregate failure rates over the initial 24-month test period.

Asset Health Indices can assist with prioritizing spares strategies and to allow adequate planning time for an asset's capital replacement. The following initial AHI for the sodium-nickel-chloride (Table 4.9) battery was developed using educated guesses based on manufacturing data and experimental test data. It is expected to improve in accuracy through back-testing as more operational data becomes available.

Table 4.9 Asset health indexes

Battery system	Assessment criteria	Score		
		0 = Poor	2 = Fair	5 = Good
Idle battery surface temp.	Over ambient [°C]	> 20	10 – 20	< 10
Battery surface temp. during discharge	Over ambient [°C]	> 30	15 - 30	< 15
Float voltage 5 min. after AC turns off (“Rest voltage”)	Assuming 129 V rated voltage [V]	< 127	127 - 129	> 129
Discharge at C/4 capacity	Assuming 80 Ah battery [Ah]	< 70	70 - 75	> 75
Discharge at C/4	Mean temperature [°C]	> 280	270 - 280	< 270
Annual number of critical alarms.	3-year moving average	≥ 3	1-3	≤ 1
Age (BMS)	Assuming 20-yr lifetime [years]	> 20	10-20	< 10
Age (Batteries)	Assuming 20-yr lifetime [years]	> 20	10-20	< 10
Discharge number	Lifetime discharges	> 2000	1000 - 2000	< 1000

In summary sodium-nickel-chloride batteries were tested on a previously untested environment, that of a substation. Its performance exceeded expectations with the batteries showing no capacity loss over 18 months. Due to their promise, an RCM-based maintenance program and asset health indexes were developed in anticipation of installing these batteries in various substations.

Chapter 5 Conclusion

The objective of this thesis was to select and test previously untested battery systems for use in substation applications. To that effect different chemistries were considered but, in the end, the two that were chosen to be tested in detail were a lithium-ion and a sodium-nickel-chloride one. This chapter highlights the contribution and the important findings of the thesis and offers recommendations for future work.

5.1 Contributions

- 1) An overview of battery fundamentals as well as battery chemistries was provided. A step by step development of a model based on simple electrical components was presented. It was found that the most efficient way to estimate the open circuit voltage was to discharge the battery at rates lower than $C/20$ and that in order to create an accurate battery model some initial experiments need to be performed. An additional model based on Shepherd equation was also developed. The results of both models seem to agree to those obtained via experiment..
- 2) An experimental setup involving a lithium-ion battery was designed and placed on a mock substation that is used for training purposes. It was found that a lithium-ion battery bank could operate the substation equipment. However, based on calendar aging results the performance of lithium-ion batteries was deemed unsatisfactory (based on an expected life of 20 years) for substation applications due to their 4-6% capacity loss over the first 18 months of operation.

- 3) An experiment that was used to accelerate the battery aging was designed and from the results it was found that the batteries that are stored at a lower SOC age more slowly. Based on that, a sizing procedure built on compounding capacity was proposed.
- 4) Sodium-nickel-chloride batteries were tested for the first time in a substation application. From the results obtained these batteries proved particularly promising, as they exhibited no measurable capacity loss over 18 months. However, it was found that their capacity is dependent on the discharge current; to that effect sizing procedures were developed.
- 5) The results for lithium-ion and sodium-nickel-chloride battery testing in substation application were published in Battcon 2018 in a paper written by the author of this thesis titled “Battery Systems in a Substation: Manitoba Hydro’s Experience with Alternative Technologies” [36].
- 6) Due to their potential as a substation battery bank the necessary background for a utility to adopt these batteries was developed, which included a maintenance framework based on RCM and health indexes. This finding together with some experimental results were published in CIGRE Canada 2018 in a paper titled “Evaluating High Energy Density Battery Technologies for Station Standby Applications” [37] written by the author of this thesis. The paper won the award for the best student paper.
- 7) Overall the objective of the theses was met with sodium-nickel-chloride being a reliable high-power density battery that can significantly lower maintenance leading to lower operating costs.

5.2 Future Work and Limitations

While sodium-nickel-chloride performed satisfactorily, a major limitation is the fact that it does not yet have a solution that is at the correct substation voltage (133 V). Due to the presence of BMSs, advanced batteries systems, such as lithium-ion and sodium -nickel-chloride, cannot be put in series to achieve the correct voltage. What this means is that the manufacturer would have to develop a product that is of the right voltage. An additional limitation is that currently there is only one manufacturer for sodium-nickel-chloride batteries; something that can have an impact in future replacement cost or product support. Furthermore, additional research will need to be done on the long term environmental impact of both technologies both from a raw material and salvage/recycle points of view.

A possible future work proposal would be to identify solutions that sodium-nickel-chloride batteries would be a good fit for and work with the manufacturer to develop a suitable implementation. Another possible extension of the work for the utilities market would be to do a station by station cost analysis of sodium-nickel-chloride batteries against the current battery implementations and the development of purchasing specification.

Of additional interest would be to evaluate sodium-nickel-chloride batteries for energy storage application and grid stability.

Last but not least, ways of artificially and non-destructively aging sodium-nickel-chloride batteries could be explored in order to help with asset management and faster development of accurate asset health indexes.

References

- [1] A. A.-H. Hussein and I. Batarseh, “An overview of generic battery models,” in *Proc. 2011 IEEE Power and Energy Society General Meeting*, 2011, pp. 1–6.
- [2] G. Liu, L. Lu, H. Fu, J. Hua, J. Li, M. Ouyang, Y. Wang, S. Xue, and P. Chen, “A comparative study of equivalent circuit models and enhanced equivalent circuit models of lithium-ion batteries with different model structures,” in *Proc. 2014 IEEE Conference and Expo Transportation Electrification Asia-Pacific (ITEC Asia-Pacific)*, 2014, pp. 1–6.
- [3] N. Koirala, F. He, and W. Shen, “Comparison of two battery equivalent circuit models for state of charge estimation in electric vehicles,” in *Proc. 2015 IEEE 10th Conference on Industrial Electronics and Applications (ICIEA)*, 2015, pp. 17–22.
- [4] M. Rahman , S. Anwar, A. Izadian (2016) Electrochemical Model Based Fault Diagnosis of Lithium Ion Battery. *Adv Automob Eng* 5: 159. doi: 10.4172/2167- 7670.1000159
- [5] S. Jiang and Shugang, “A Parameter Identification Method for a Battery Equivalent Circuit Model,” in *SAE Technical Paper*, 2011, no. 2310, pp. 1–9.
- [6] R. Xiong, H. He, H. Guo, and Y. Ding, “Modeling for Lithium-Ion Battery used in Electric Vehicles,” *Procedia Eng.*, vol. 15, pp. 2869–2874, 2011.
- [7] J. Vetter, P. Novák, M. R. Wagner, C. Veit, K.-C. Möller, J. O. Besenhard, M. Winter, M. Wohlfahrt-Mehrens, C. Vogler, and A. Hammouche, “Ageing mechanisms in lithium-ion batteries,” *J. Power Sources*, vol. 147, no. 1–2, pp. 269–281, Sep. 2005.

- [8] M. Broussely, P. Biensan, F. Bonhomme, P. Blanchard, S. Herreyre, K. Nechev, and R. J. Staniewicz, "Main aging mechanisms in Li ion batteries," *J. Power Sources*, vol. 146, no. 1–2, pp. 90–96, Aug. 2005.
- [9] I. Buchmann, *Batteries in a portable world: a handbook on rechargeable batteries for non-engineers.*, Cadex Electronics Inc., second edition 2001
- [10] J. Schmalstieg, S. Kabitz, M. Ecker, and D. U. Sauer, "From accelerated aging tests to a lifetime prediction model: Analyzing lithium-ion batteries," in *Proc. 2013 World Electric Vehicle Symposium and Exhibition (EVS27)*, 2013, pp. 1–12.
- [11] M. Lewerenz, J. Münnix, J. Schmalstieg, S. Käbitz, M. Knips, and D. U. Sauer, "Systematic aging of commercial LiFePO₄|Graphite cylindrical cells including a theory explaining rise of capacity during aging," *J. Power Sources*, vol. 345, pp. 254–263, Mar. 2017.
- [12] M. Hosseinfar and A. Petric, "High temperature versus low temperature Zebra (Na/NiCl₂) cell performance," *J. Power Sources*, vol. 206, pp. 402–408, May 2012.
- [13] M. Leksell et al "Long-Term Field Experience with a Stationary Lithium-Ion Battery in a Sub-Station Application", Proceedings of Battcon 2011
- [14] P. Krohn, , B. Nygren, T. Beyer, "Field experience from the world's largest stationary Lithium-ion battery", Proceedings of Battcon 2007
- [15] R. Benato, S. D. Sessa, G. Crugnola, M. Todeschini, and S. Zin, "Sodium nickel chloride cell model for stationary electrical energy storage," in *Proc. 2015 AEIT International Annual Conference (AEIT)*, 2015, pp. 1–6.
- [16] IEEE Std 446-1995 [The Orange Book] : IEEE Recommended Practice for Emergency and Standby Power Systems for Industrial and Commercial Applications. IEEE, 1996.

- [18]K. S. Ng, C.-S. Moo, Y.-P. Chen, and Y.-C. Hsieh, “Enhanced coulomb counting method for estimating state-of-charge and state-of-health of lithium-ion batteries,” *Appl. Energy*, vol. 86, no. 9, pp. 1506–1511, Sep. 2009.
- [19]D. Doerffel and S. A. Sharkh, “A critical review of using the Peukert equation for determining the remaining capacity of lead-acid and lithium-ion batteries,” *J. Power Sources*, vol. 155, no. 2, pp. 395–400, Apr. 2006.
- [20]“BU-503: How to Calculate Battery Runtime – Battery University.” [Online]. Available: https://batteryuniversity.com/learn/article/bu_503_how_to_calculate_battery_runtime. [Accessed: 05-Nov-2018].
- [21] J. Kim, “Battery fundamentals”, Battcon 2017, Orlando, FL, 2017
- [22] B. Chamala, “Focus on: Advanced Battery Technologies”, Battcon 2018, Nashville, TN, 2018
- [23]I. Buchmann, *Batteries in a portable world: a handbook on rechargeable batteries for non-engineers*. Cadex Electronics Inc., 2011.
- [24]G. Plett, *Battery Management Systems, Volume I*. Artech House, 2015
- [25]E. Raszmann, K. Baker, Y. Shi, and D. Christensen, “Modeling stationary lithium-ion batteries for optimization and predictive control,” in *2017 IEEE Power and Energy Conference at Illinois (PECI)*, 2017, pp. 1–7. 5.
- [26]L.G. Debin et.al, “Station control DC system criteria review report”, Manitoba Hydro internal report, Winnipeg, MB, 2004
- [27] J. McDowall, “Lithium Ion Technology,” Battcon 2018, Nashville, TN, 2018.

- [28] H.-G. Schweiger, O. Obeidi, O. Komesker, A. Raschke, M. Schiemann, C. Zehner, M. Gehnen, M. Keller, and P. Birke, "Comparison of Several Methods for Determining the Internal Resistance of Lithium Ion Cells," *Sensors*, vol. 10, no. 12, pp. 5604–5625, Mar. 2010.
- [29] L. Bodenes, et al. "Lithium secondary batteries working at very high temperature: Capacity fade and understanding of aging mechanisms" , *J. Power Sources* 236, 265–275, 2013.
- [30]] M. Lewerenz, J. Münnix, J. Schmalstieg, S. Käbitz, M. Knips, and D. U. Sauer, "Systematic aging of commercial LiFePO₄|Graphite cylindrical cells including a theory explaining rise of capacity during aging," *J. Power Sources*, vol. 345, pp. 254–263, Mar. 2017.
- [31] A. Miraldi, "FZSoNick Sodium Nickel Batteries", FZSoNick Manitoba hydro in house presentation, Winnipeg, MB, 2018
- [32] Nowlan, Heap & United Air Lines Inc San Francisco Ca," Reliability-Centered Maintenance.", California, 1978.
- [33] A. K. Miraldi, "Sodium Metal Chloride Battery Quarter Life Capacity Testing and Field Results", Battcon 2017, Orlando, FL, 2017
- [34] J. Schmalstieg, S. Kabitz, M. Ecker, and D. U. Sauer, "From accelerated aging tests to a lifetime prediction model: Analyzing lithium-ion batteries," in *Proc. 2013 World Electric Vehicle Symposium and Exhibition (EVS27)*, 2013, pp. 1–12.
- [35] Qi, Zhaoxiang; Koenig, Gary M. (2017-05-12). "Review Article: Flow battery systems with solid electroactive materials". *Journal of Vacuum Science & Technology B, Nanotechnology and Microelectronics: Materials, Processing, Measurement, and Phenomena*.
- [36] K. Stamatis et.al, "Battery Systems in a Substation: Manitoba Hydro's Experience with Alternative Technologies", Battcon 2018, Nashville, TN, 2018.

- [37] K. Stamatis et.al, “Evaluating High Energy Density Battery Technologies for Station Standby Applications”, CIGRE Canada 2018, Calgary, AB, 2018.
- [38] S. McCluer,” Battery Technology for Data Centers and Network Rooms: Lead-Acid Battery Options”, White paper 30, 2011.
- [39] IEEE Recommended Practice for Maintenance, Testing, and Replacement of Vented Lead-Acid Batteries for Stationary Applications," in IEEE Std 450-2010 (Revision of IEEE Std 450-2002) , vol., no., pp.1-71, 25 Feb. 2011.
- [40] IEEE Recommended Practice for Sizing Lead-Acid Batteries for Stationary Applications," in IEEE Std 485-2010 (Revision of IEEE Std 485-1997) , vol., no., pp.1-90, 15 April 2011.
- [41]NERC, “Protection System Maintenance PRC-005-2” , www.nerc.com/files/PRC-005-2.pdf, 2007,[1/7/2019]